第 25 卷第 5 期 无 机 化 学 学 报 Vol.25 No.5
2009 年 5 月 CHINESE JOURNAL OF INORGANIC CHEMISTRY 900~905

多阴离子和铜磷酸盐为基元的杂化材料的合成、结构和性质

赵志凤[1] 周百斌*,[1,2] 苏占华[1,2] 朱春城[2]
([1]哈尔滨工业大学化工学院,哈尔滨 150001)
([2]哈尔滨师范大学化学化工学院,哈尔滨 150025)

摘要:本文采用水热法合成了一个新的金属有机-无机杂化化合物 $[Cu_4(phen)_4(HPO_4)_2(H_2O)_2(OH)_2][HPMo_{12}O_{40}]\cdot H_2O$ (**1**) (phen=邻菲咯啉)。通过元素分析、红外光谱、热重分析、X-射线单晶衍射对其进行了结构表征。化合物 **1** 是由四核铜磷酸盐、Keggin 阴离子和晶格水分子组成。四核铜磷酸盐和多阴离子之间通过弱的 M…O 相互作用形成二维结构(M=Cu, Mo), 该二维结构通过氢键和 π-π 相互作用形成三维超分子框架,还对化合物 **1** 的电化学和电催化性质进行了研究。

关键词:水热合成;晶体结构;多金属氧酸盐;电化学
中图分类号:O614.121;O614.61+2 **文献标识码**:A **文章编号**:1001-4861(2009)05-0900-06

Synthesis, Structure and Properties of A Hybrid Material Based on Polyoxoanion and Copper Phosphate

ZHAO Zhi-Feng[1] ZHOU Bai-Bin*,[1,2] SU Zhan-Hua[1,2] ZHU Chun-Cheng[2]
([1]*School of Chemical Engineering and Technology, Harbin Institute of Technology, Harbin* 150001)
([2]*Institute of Chemistry and Chemical Engineering, Harbin Normal University, Harbin* 150025)

Abstract: A new metalorganic-inorganic hybrid compound $[Cu_4(phen)_4(HPO_4)_2(H_2O)_2(OH)_2][HPMo_{12}O_{40}]\cdot H_2O$ (**1**) (phen =1,10-phenanthroline), has been hydrothermally synthesized and structurally characterized by elemental analysis, IR spectrum, thermal analysis and single-crystal X-ray structural analysis. Compound **1** is consisted of a tetranuclear copper phosphate $[Cu_4(phen)_4(HPO_4)_2(H_2O)_2(OH)_2]^{2+}$, Keggin polyoxoanion $[HPMo_{12}O_{40}]^{2-}$ and the lattice water molecule. Compound **1** generates an interesting 2D network between the tetranuclear copper phosphates and polyoxoanions by weak M…O interactions (M=Cu, Mo), which is further connected into a 3D supramolecular architecture through hydrogen bonds and π-π interactions. Compound **1** was used as a solid bulk modifier to fabricate a carbon paste electrode (1-CPE) by direct mixing. The electrochemical and electrocatalytic behaviors of the 1-CPE have been studied in detail. CCDC: 666620.

Key words: hydrothermal synthesis; crystal structure; polyoxometalates; electrochemistry

0 Introdution

Polyoxometalates (POMs), as one kind of significant metal-oxygen cluster, have been employed as inorganic building blocks for construction of solid state materials with various metal-organic coordination polymers because of not only their intriguing structural diversity but also potential applications in catalysis,

收稿日期:2008-09-09。收修改稿日期:2009-04-07。
国家自然科学基金资助项目(No.20371014,20671026)。
*通讯联系人。E-mail:zhou_bai_bin@163.com
第一作者:赵志凤,女,29 岁,博士研究生;研究方向:多酸化学。

biochemical analysis, medicinal chemistry, and materials science[1]. Transition metal phosphates have also received considerable attention for their widespread applications in the fields of catalysis, separation, adsorption and host-guest assembly[2]. Our group has been attempting to incorporate POMs into transition metal phosphates and to explore the synergistic reaction between them. One of the important targets in the preparation hybrid materials of based on transition metal phosphates and POMs is to establish the possible connections between organic and/or inorganic molecular fragments by various forces including strong and directional interactions[3] (e.g. metal-ligand bonding) and weak interactions, such as hydrogen-bonding[4], π-π stacking[5], CN$\cdots\pi$ interaction and CN$\cdots$Cu interaction[6], weak Cu$\cdots$X (X=O, Br) interaction[7], halogen-halogen[8], Ag$\cdots$X (X=Ag, O, S) interactions[9], Br$\cdots\pi$ interaction[10], and so on. The weak interactions are extremely important in the construction of high dimensional networks. Recently, several crystal structures based on transition metal phosphates and POMs have been synthesized, for example, cobalt phosphonate hybrid material[11], polyoxomolybdate clusters into copper phosphonate network[12]. However, the construction networks of based on transition metal phosphates and POMs through weak metal-oxygen interactions remains is a great challenge. Therefore, we are appealed in the study of the weak interactions and their influence on packing styles. Herein, we report the synthesis, structure, thermal properties, electrochemical and electrocatalytic properties of $[Cu_4(phen)_4(HPO_4)_2(H_2O)_2(OH)_2][HPMo_{12}O_{40}]\cdot H_2O$.

1 Experimental

1.1 Materials and physical measurements

All reagents were purchased commercially and used without further purification. Elemental analyses (C, H, and N) were performed on a Perkin-Elmer 2400 CHN Elemental Analyzer. The infrared spectra were obtained on a Nicolet Impact 410 FTIR spectrometer in the 400~4 000 cm^{-1} region with pressed KBr pellets. Thermogravimetric analyses were recorded in a dynamic nitrogen atmosphere with a heating rate of 10 ℃·min^{-1} using a Mettler TGA/SDTA851e thermal analyzer. Electrochemical measurements were made on a CHI 660b electrochemical workstation. A conventional three-electrode system was used. The working electrode was a modified carbon paste electrode (CPE). Ag/AgCl (3 mol·L^{-1} KCl) electrode was used as a reference electrode and a Pt wire as a counter electrode.

1.2 Synthesis

A mixture of $CuSO_4\cdot 5H_2O$ (1.28 mmol), $Na_2MoO_4\cdot 2H_2O$ (2.48 mmol), H_3PO_4 (7.34 mmol), 1,10-phenanthroline (0.28 mmol), and H_2O (7.0 mL) was stirred for 80 min in air, The mixture was then transferred to a 20 mL Teflon-lined autoclave and kept 160 ℃ for 6 days under autogenous pressure, after cooling to room temperature. The green block crystals of **1** were washed with distilled water, and dried at ambient temperature (yield: 35% based on Mo). Calcd for $C_{48}H_{43}N_8O_{53}Cu_4Mo_{12}P_3$ (%): C 18.73, H 1.41, N 3.64. Found (%): C 18.65, H 1.46, N 3.57. IR(KBr, cm^{-1}): 3 425(s), 1 610(m), 1 427(m), 1 057 (vs), 994(vs), 846(s), 739(m).

1.3 X-ray crystal structural analysis

Diffraction data of **1** were collected on a Bruker SMART CCD diffractometer using graphite monochromatic Mo $K\alpha$ radiation (λ=0.071 073 nm) at 293(2) K. A total of 13 738 reflections were collected in the range of $1.92°\leqslant\theta\leqslant 28.29°$, of which 9 270 reflections were unique with R_{int}=0.025 1 and 7 430 with $I>2\sigma(I)$ were considered as observed. The structure was solved by direct methods and refined by the full-matrix least-squares methods on F^2, which were performed using the SHELX-97 software package[13,14]. The final R_1 and wR_2 were 0.034 3 and 0.073 7. All non-hydrogen atoms were refined anisotropically and hydrogen atoms on carbon atoms were included at calculated positions and refined with a ring model, hydrogen atoms on water molecule (O1W) were left out and hydrogen atoms attached to water molecule (O27) were located from the Fourier maps. The crystal data and structure refinement parameters of compound **1** were summarized in Table 1. Selected bond lengths and angles were listed in Table 2.

CCDC: 666620.

Table 1 Crystal data and structure refinement parameters for 1

Empirical formula	$C_{48}H_{43}Cu_4Mo_{12}N_8O_{53}P_3$	D_c / (g·cm^{-3})	2.685
Formula weight	3 078.25	μ (Mo $K\alpha$) / mm^{-1}	3.173
Crystal system	Triclinic	F(000)	1 476
Space group	$P\bar{1}$	Crystal size / mm	0.22×0.17×0.15
a / nm	1.065 47(2)	θ range/ (°)	1.92~28.29
b / nm	1.425 00(4)	Reflections collected / unique	13 738
c / nm	1.438 78(4)	Independent reflections (R_{int})	9 270 (0.025 1)
β / (°)	85.631(2)	GOF on F^2	1.061
Volume / nm^3	1.903 86(8)	Final R indices [$I>2\sigma(I)$]	R_1=0.034 5, wR_2=0.074 3
Z	1	R indices (all data)	R_1=0.049 7, wR_2=0.084 5

Table 2 Selected bond lengths (nm) and angles (°) for 1

Mo(1)-O(5)	0.166 6(4)	Mo(2)-O(10)	0.184 9(5)	Mo(1)-O(2)	0.184 0(4)
Mo(2)-O(1)	0.194 1(5)	Mo(3)-O(13)	0.198 2(4)	Mo(3)-O(2)	0.197 5(4)
Mo(4)-O(18)	0.195 7(4)	Mo(5)-O(15)$^{\#1}$	0.197 1(5)	Mo(4)-O(12)	0.250 0(6)
Mo(5)-O(17)$^{\#1}$	0.248 3(6)	Mo(6)-O(4)	0.185 5(4)	Mo(6)-O(22)	0.166 2(4)
Cu(1)-O(23)	0.196 9(3)	Cu(2)-O(27)	0.196 2(4)	Cu(1)-N(1)	0.201 8(4)
Cu(2)-N(4)	0.199 4(4)	P(2)-O(24)$^{\#2}$	0.153 0(3)	P(1)-O(6)	0.153 5(6)
O(5)-Mo(1)-O(2)	102.9(2)	O(9)-Mo(2)-O(10)	93.6(2)	O(3)-Mo(1)-O(7)	91.2(2)
O(11)-Mo(2)-O(12)	159.4(2)	O(16)-Mo(3)-O(13)	99.9(2)	O(14)-Mo(3)-O(13)	155.6(2)
O(20)-Mo(4)-O(8)	102.5(2)	O(3)-Mo(5)-O(18)$^{\#1}$	94.6(2)	O(13)-Mo(4)-O(19)	155.9(3)
O(21)-Mo(5)-O(9)	101.0(2)	O(22)-Mo(6)-O(7)	159.3(2)	O(4)-Mo(6)-O(12)$^{\#1}$	94.5(2)
N(1)-Cu(1)-O(25)	89.78(16)	O(27)-Cu(2)-N(4)	90.35(17)	O(24)-Cu(1)-O(25)	98.06(15)
N(4)-Cu(2)-N(3)	82.55(16)	O(26)-P(2)-O(28)	109.2(2)	O(7)-P(1)-O(6)	68.5(3)

Symmetry transformations used to generate equivalent atoms: $^{\#1}$ $-x+1, -y+1, -z$; $^{\#2}$ $-x+2, -y+1, -z+1$.

2 Results and discussion

2.1 Structure description

The single crystal structure revealed that **1** is consisted of copper phosphate $[Cu_4(phen)_4(HPO_4)_2(H_2O)_2(OH)_2]^{2+}$ as the metal-organic one, Keggin polyoxoanion $[PMo_{12}O_{40}]^{3-}$ as the inorganic building and lattice water molecule (Fig.1), moreover, one free proton may be located at polyoxoanion serving as counterion in **1**. In the well-known Keggin structure, there are 12 $\{MoO_6\}$ octahedra and one PO_4 tetrahedron. The 12 $\{MoO_6\}$ are arranged in four groups of three edge-shared octahedra $\{Mo_3O_{16}\}$, which are joined to each other by sharing corners. According to the different coordination fashion of O atoms in Keggin anion, the Mo-O bond lengths can be classified into three sets: Mo-O_t, 0.164 7(4)~0.166 6(4) nm; Mo-O_b, 0.183 3(4)~0.198 4(4) nm; Mo-O_i, 0.241 6(5)~0.250 9(6) nm, while the coordination bond angles at the Mo centers are in the range of 40.39(18)°~161.8(2)°. The central P atom is surrounded by a cube of eight oxygen atoms with each oxygen site half-occupied[12]. The P(1)-O distances are in the range of 0.148 6(5)~0.156 2(6) nm and O-P(1)-O angles 68.3(3)°~180.0(4)°.

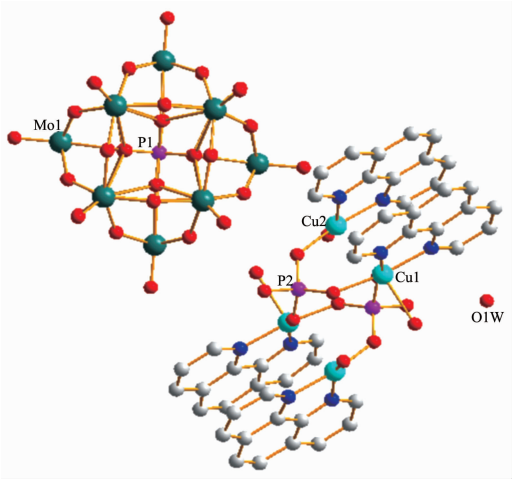

Fig.1 Molecular structure of **1**

$[Cu_4(phen)_4(HPO_4)_2(H_2O)_2(OH)_2]^{2+}$ serves as the cation, with butterfly topology. The cation itself may be considered as a type of organic-inorganic hybrid material with the organoamine ligands directly coordinated to the scaffolding. Two types of Cu species, indicated as Cu(1) and Cu(2), respectively, which are crystallographically independent. Each Cu atom has square pyramidal geometry with N_2O_3 donor set. The two $[CuN_2O_3]$ are interlinked by the bridging oxygen atoms from HPO_4 ligands. The four basal positions are occupied by two N atoms of the phen ligand and two phosphate oxygen atoms, the Cu-N distances are in the range of 0.199 4(4)~0.202 1(4) nm, the basal Cu-O bond lengths range from 0.193 3(3) to 0.196 9(3) nm, and the coordination sphere at the apical position of Cu(1) is a hydroxide (Cu(1)-O(25) 0.225 6(4) nm) and Cu(2) is completed by a terminal coordinated water molecular(Cu(2)-O(27) 0.196 2(4) nm). Bonding about Cu(1) varies with donor type and position with apical bond lengths significantly longer than the basal-plane ones, as might be anticipated by the Jahn-Teller theorem. Distance of Cu(1)···Cu(2) is 0.326 1 nm and 0.439 0 nm, respectively. P(2) makes three bonds to Cu atoms with P-O distances 0.152 4(4)~0.158 1(4) nm, terminal P-OH bond as its fourth vertex [dP(2)-O(28)= 0.158 1(4) nm]. Valence sum calculations[15] reveal that in **1**, all Mo centers are +6 oxidation states ($\sum s$ =6.18~6.26), the P sites are +5 oxidation states ($\sum s$=4.93~4.99), the Cu sites are +2 oxidation ($\sum s$=1.72~1.77) states.

It is noteworthy that the structure of **1** exhibits weak interactions between tetranuclear copper phosphates and the Keggin anions [(Cu(2)···O(5)=0.279 2 nm, Mo(6)···O(27)=0.361 4 nm)], forming a two-dimension network (Fig.2), different from that of polyoxianions linked transition metals with strong coordination interaction or only electrostatic interaction in previous literature[16]. Although such kind of copper-oxygen distance is considerably long beyond the range of coordination interaction, it is less than the sum of van der Waals radii of copper and oxygen (0.355 nm), and Mo···O distance is close to the sum of van der Waals radii of molybdenum and oxygen (0.365 nm)[17]. On account of the weaker Cu···O and Mo···O interactions, the packing of **1** can be described as an extended framework constructed from polyoxoanions attached by tetranuclear copper phosphates linkages.

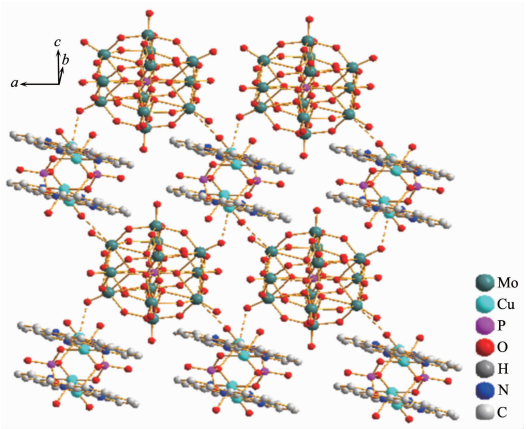

Fig.2　Ball-and-stick representation of the 2D network of **1** by the weaker Cu···O and Mo···O interactions

There is an intramolecular H-bonding between the apical coordinated water molecule O(27) and phosphate oxygen O(24) [O(27)–H27A···O(24) 0.269 3(6) nm]. Intermolecular H-bonding contacts are observed between water molecules and/or hydroxyl and the oxo groups of polyoxoanions (Table 3). In addition to π-π interactions are also found between benzene rings from phen ligands and play an important role in stabilizing the network. Furthermore, the 2D networks were

Table 3　Distances and angles of hydrogen bonding for 1

D–H···A	*d*(D-H) / nm	*d*(H···A) / nm	*d*(D···A)/nm	∠(DHA) / (°)
O(25)–H(25)···O(13)$^{\#1}$	0.082	0.256	0.293 7(6)	109.2
O(27)–H(27A)···O(24)	0.075(7)	0.202(7)	0.269 3(6)	150(7)
O(27)–H(27A)···O(22)$^{\#2}$	0.075(7)	0.245(7)	0.281 7(5)	112(6)
O(27)–H(27B)···O(14)$^{\#2}$	0.077(9)	0.263(9)	0.322 5(6)	135(8)
O(28)–H(28)···O(1W)	0.082	0.210	0.284 0(7)	150.4
O(28)–H(28)···O(11)$^{\#1}$	0.082	0.254	0.301 9(5)	118.3

Symmetry transformations used to generate equivalent atoms: $^{\#1}$ $-x+1, -y+1, -z+1$; $^{\#2}$ $x+1, y, z+1$.

stacked by H-bonding and π-π interactions to form a 3D supramolecular architecture.

2.2 TG analysis

Thermogravimetric analysis (TGA) also supports the chemical composition. In the TG curve of **1** (Fig.3), there exist two weight loss stages. In the temperature range of 165~235 ℃, the initial weight loss of 2.97% corresponds to the release of water molecule (calcd 2.89%). The second weight loss of 23.96% occurring between 400 ℃ and 490 ℃ is release of the phen ligands (23.42%). The whole weight loss (26.93%) is in good agreement with the calculated value (26.31%).

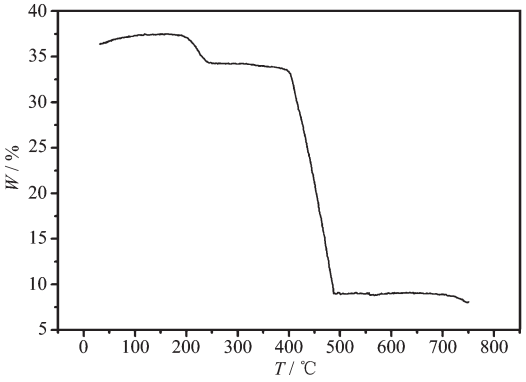

Fig.3 TG curve of **1**

2.3 Voltammetric behavior of 1-CPE

The cyclic voltammograms for 1-CPE in 1 mol·L^{-1} H_2SO_4 aqueous solution at different scan rates is presented in Fig.4. There are three pairs of reversible redox peaks appear in the potential range of +700 to −100 mV. The half-wave potentials $E_{1/2}=(E_{cp}+E_{ap})/2$ are +490, +372 and +226 mV, respectively. The three redox peaks can be ascribed to redox process of molybdenum[18]. The fourth irreversible anodic peak(Ⅳ) is assigned to the oxidation of Cu^{2+} at 128 mV[19].

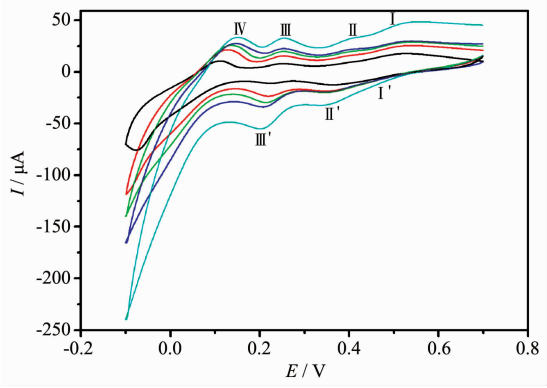

From inner to outer: 20, 50, 80, 110, 140 mV·s^{-1}

Fig.4 Cyclic voltammograms of the 1-CPE in 1 mol·L^{-1} H_2SO_4 at different scan rates

When the scan rate was varied from 20 to 140 mV·s^{-1}, the catholic peak potentials shift towards the negative direction and the corresponding anodic peak potentials to the positive direction with increasing scan rates. The peak to peak separation between the corresponding cathodic and anodic peaks increases with the scan rate increasing, but the mean peak potentials do not change on the whole. This may be explained as the following: the reduction of the compound immobilized in the CPE is accompanied by the evolution of protons from solution to maintain charge neutrality, while the encapsulation of the compound may slow down the penetration rate of protons and decrease the electron exchange rate to some extent.

2.4 Electrocatalytic reduction of nitrite on 1-CPE

As is known, POMs have been exploited extensively in electrocatalytic reductions[20]. Dong and Keita et al. have reported the electrocatalytic reduction of NO_2^- with $SiW_{12}O_{40}^{4-}$ and POMs/polymer system, respectively[21]. In our experiment, we found compound **1** bulk-modified CPE also displayed excellent electrocatalytic activity toward the reduction of NO_2^- in 1 mol·L^{-1} H_2SO_4 in the range +700 to −100 mV, as shown in Fig.5. It can be seen that with the addition of NO_2^-, the peak-to-peak separations between the corresponding anodic and cathodic peaks increase, the reduction peak

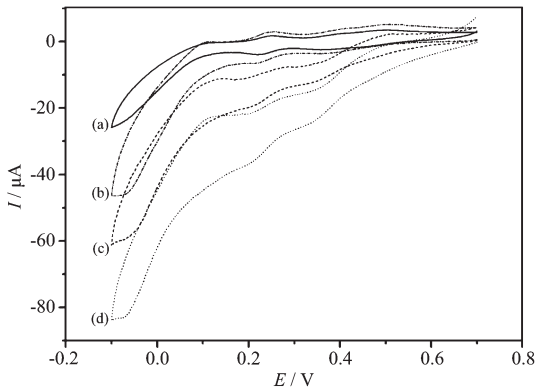

Scan rate: 15 mV·s^{-1}

Fig.5 Cyclic voltammograms of the 1-CPE in 1 mol·L^{-1} H_2SO_4 containing (a) 0; (b) 3.8; (c) 7.5; (d) 15 mmol·L^{-1} $NaNO_2$

currents at negative domain increase remarkably while the corresponding oxidation peak currents decrease, suggesting that the 1-CPE has good electrocatalytic activities toward the reduction of nitrite.

3 Conclusions

In summary, we have prepared and structurally characterized a novel 2D network formed by the weaker M…O interactions of polyoxoanions and tetranuclear copper phosphates, which confirms the utility of weaker M…O interactions for the synthesis of structural organic-inorganic hybrid solid state materials (M=Cu, Mo). The electrochemical and electrocatalytic behaviors of the 1-CPE have been studied in detail.

References:

[1] Hill C L. *Chem. Rev.*, **1998**,**98**(1):1~2

[2] Yang G Y, Sevov S C. *J. Am. Chem. Soc.*, **1999**,**121**(36):8389~8390

[3] Tong M L, Wu Y M, Ru J, et al. *Inorg. Chem.*, **2002**,**41**(19):4846~4848

[4] WANG Xiang(王　祥), LUO Fang(罗　芳), GAO Wei-Tao(高文涛). *Chinese J. Inorg. Chem.*(*Wuji Huaxue Xuebao*), **2009**, **25**(1):154~157

[5] LU Zhen-Da(鲁振达), YAO Jing(姚　景), LIN Jian-Guo(林建国), et al. *Chinese J. Inorg. Chem.* (*Wuji Huaxue Xuebao*), **2008**,**24**(8):1335~1342

[6] Stephenson M D, Hardie M J. *Cryst. Growth. Des.*, **2006**,**6**(2):423~432

[7] Li T H, Lü J, Gao S Y, et al. *Inorg. Chem. Commun.*, **2007**,**10**(5):551~554

[8] Matsumoto A, Tanaka T, Tsubouchi T, et al. *J. Am. Chem. Soc.*, **2002**,**124**(30):8891~8902

[9] Xie Y B, Li J R, Bu X H. *Polyhedron*, **2005**,**24**(3):413~418

[10]Rosokha Y S, Lindeman S V, Rosokha S V, et al. *Angew Chem. Int. Ed*, **2004**,**43**(35):4650~4652

[11]Yuan M, Li Y G, Wang E B, et al. *J. Chem. Soc. Dalton. Trans.*, **2002**,**14**:2916~2920

[12]Lu Y, Wang E B, Guo Y Q, et al. *J. Mol. Struct.*, **2005**,**737**(2~3):183~187

[13]Sheldrick G M. *SHELXS*-97, *Program for Crystal Structure Solution*, University of Göttingen, Germany, **1997**.

[14]Sheldrick G M. *SHELXL*-97, *Program for Crystal Structure Refinement*, University of Göttingen, Germany, **1997**.

[15]Brese N E, O′Keeffe M. *Acta Crystallogr. Sect. B*, **1991**,**47**:192~197

[16]Sun C Y, Li Y G, Wang E B, et al. *Inorg. Chem.*, **2007**,**46**(5):1563~1574

[17]Batsanov S S. *Inorg. Mater.*, **2001**,**37**(9):871~885

[18]Han Z G, Zhao Y L, Peng J, et al. *Electroanalysis*, **2005**,**17**(12):1097~1102

[19]Zhao Z F, Zhou B B, Su Z, et al. *Inorg. Chem. Commun.*, **2008**,**11**(6): 648~651

[20]Toth J E, Anson F C. *J. Electroanal. Chem.*, **1988**,**256**(2):361~370

[21]Keita B, Belhouari A, Nadjo L, et al. *J. Electroanal. Chem.*, **1995**,**381**(1~2):243~250